On the Low-Lying States and Electronic Spectroscopy of Iron(II) Porphine

W. Daniel Edwards,† Brian Weiner, and Michael C. Zerner*

Contribution from the Quantum Theory Project, University of Florida, Gainesville, Florida 32611, and the Guelph Waterloo Centre for Graduate Work in Chemistry, University of Guelph, Guelph, Ontario, Canada N1G2W1. *Received October 10, 1985*

Abstract: Calculations are made on the low-lying electronic states of iron(II) porphine. Although these calculations yield the $^3A_{2g}$ state as lowest, an argument is presented in favor of the ^3E_g state calculated to lie some 240 cm^{-1} higher in energy. A detailed discussion of these results in conjunction with various seemingly conflicting experimental and theoretical results is made. The UV visible spectra is computed assuming each of five possible ground states, $^1A_{1g}$, $^3A_{2g}$, ^3E_g, ^5E_g, $^5A_{1g}$, and ^5E_g. The calculated spectra from the $^3A_{2g}$ and ^3E_g states are in good accord with experiment, and we argue that the extra bands observed at 12 500 and 15 000 cm^{-1} are due to trip-triplets, porphyrin $\pi \rightarrow \pi^*$ triplets that have gained intensity by spin coupling with the iron atom triplet state. The calculated charge-transfer and d $\rightarrow$ d spectra are described and are compared with other calculations. Although d $\rightarrow$ d states are predicted to lie below the Q band they are either spatially or spin forbidden and might be difficult to observe. We do not calculate any charge-transfer excitations below the Q band in contrast to the calculations of others.

1. Introduction

Few large molecules have enjoyed such popularity among theorists as the porphyrins. Perhaps foremost in popularity are the iron porphyrins, which are at the heart of oxygen transport in hemoglobin and myoglobin and are of central importance in electron-transfer processes throughout biology.

1. Introduction Few large molecules have enjoyed such popularity among theorists as the porphyrins. Perhaps foremost in popularity are the iron porphyrins, which are at the heart of oxygen transport in hemoglobin and myoglobin and are of central importance in electron-transfer processes throughout biology.

Although the naturally occurring iron porphyrin systems have very little symmetry, theoretical studies have primarily focused on symmetric model compounds such as shown in Figure 1. These idealized systems all have in common an extended π system and a central weakly coupled transition-metal ion and have led to more studies than we could profitably review here. However, in spite of this intense scrutiny, many basic questions still remain unanswered. For example, the ground state of the simplest model compound, that of D_{4h} iron(II) porphine (porphinatoiron(II)) or Fe(II)P remains controversial.[1-4]

In view of the interest in these systems and their obvious biological importance, we reexamine the ground state of Fe(II)P using intermediate neglect of differential overlap techniques[5-9] and compare these results with experimental and theoretical results of others. In addition, we examine the UV-visible electronic excitations that are possible assuming different ground-state symmetries. It was hoped that these calculated spectra might prove different enough to allow us to differentiate between the possible group states. Unfortunately we find that the calculated spectra of either of the two controversial low-lying triplets (intermediate spin) of $^3A_{2g}$ or ^3E_g symmetry or the low-lying quintet states (high spin) will fit the observed UV-visible spectrum. In either case, the two additional bands, characteristic of this system, observed at about 12 500 and 15 000 cm^{-1}[10] we assign to trip-triplets or trip-quintets, triplets of the porphyrin system that become spin allowed by spin coupling with the Fe(II) triplet or quintet d orbital configuration.[11,12] This spin coupling will be discussed in depth in section 5.

In the next section we describe briefly the methodology that we use in these calculations and its shortcomings. In section 4 we review the more recent ground-state calculations on this system and contrast them with those of our own. We also compare these calculated results with some of the more recent experimental findings. In section V we present calculated results for low-lying d $\rightarrow$ d, charge-transfer, and ligand-ligand transitions from the possible low-lying states of singlet, triplet, and quintet multiplicities.

2. Methodology

The calculations that we performed on these systems were of the intermediate neglect of differential overlap (INDO) type.[5-9] Self-consistent field calculations (SCF) were performed on each of the seven low-lying states reported in Table II by using a generalized open-shell operator described elsewhere.[13] The SCF calculations were then followed by a configuration interaction (CI) calculation using a Rumer diagram technique.[14-17] The oscillator strengths are evaluated with the dipole length operator, maintaining all one-center charge and polarization terms. The inclusion of the "bond" terms in this evaluation seems to have little effect on the calculated oscillator strengths.[18]

Consistent with the parameterization of this model Hamiltonian, only single excitations were included in each of the CIs. Previous studies have shown that the inclusion of double excitations lowers the calculated energy of the Soret band (near UV) and reduces its oscillator strength, yielding results in better agreement with experiment, but does not change the overall features of the cal-

* University of Florida.
† Current address: Chemistry Department, University of New Hampshire, Durham, NH 03824.

(1) Kobayashi, H.; Yanegawa, Y. *Bull. Chem. Soc. Jpn.* **1972**, *45*, 450.
(2) Hussain, S. M.; Jones, J. G. *Inorg. Nucl. Chem. Lett.* **1974**, *10*, 105.
(3) Collman, J. P.; Reed, C. A. *J. Am. Chem. Soc.* **1973**, *95*, 2048.
(4) Collman, J. P.; Hoard, J. L.; Kim, N.; Lang, G.; Reed, C. A. *J. Am. Chem. Soc.* **1975**, *97*, 2676.
(5) Pople, J. A.; Beveridge, D. L.; Dobush, P. *J. Chem. Phys.* **1967**, *47*, 2026.
(6) Ridley, J. E.; Zerner, M. C. *Theor. Chim. Acta* **1973**, *32*, 111.
(7) Ridley, J. E.; Zerner, M. C. *Theor. Chim. Acta* **1976**, *42*, 223.
(8) Bacon, A. D.; Zerner, M. C. *Theor. Chim. Acta* **1979**, *53*, 21.
(9) Zerner, M. C.; Loew, G. H.; Kirchner, R. F.; Mueller-Westerhoff, U. T. *J. Am. Chem. Soc.* **1980**, *102*, 589.
(10) Brault, D.; Rongee, M. *Biochemistry* **1974**, *13*, 4598.
(11) The notation is that of: Ake, R.; Gouterman, M. *Theor. Chim. Acta* **1969**, *15*, 20.
(12) Gouterman, M. *The Porphyrins*: Dolphin, D., Ed.; Academic: New York, 1978; Vol. III.
(13) Edwards, W. D.; Zerner, M. C., in preparation.
(14) Pauncz, R. *Spin Eigenfunctions*; Plenum: New York, 1979.
(15) Rumer, G.; Teller, E.; Weyl, H. *Gïtinger Nochr.* **1932**, *3*, 449.
(16) Cooper, I. L.; McWeeney, R. *J. Chem. Phys.* **1966**, *45*, 226. Sutcliff, B. T. *J. Chem. Phys.* **1966**, *45*, 235.
(17) McKelvey, J.; Edwards, W. D.; Zerner, M. C., in preparation. The algorithm used is that of: Reeves, C. *Commun. A. C. M.* **1966**, *9*, 276.
(18) McKelvey, J.; Zerner, M. C., unpublished.
(19) Anderson, W. P.; Edwards, W. D.; Zerner, M. C., submitted for publication.

0002-7863/86/1508-2196$01.50/0

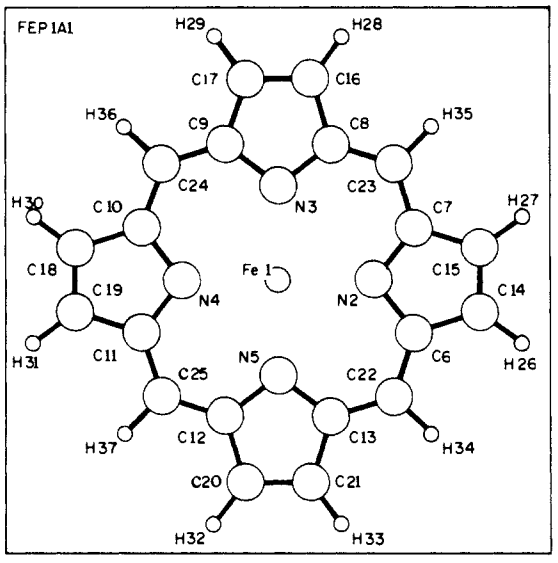

Figure 1. D_{4h} Fe(II) porphine (porphinatoiron(II)).

Table I. Structure of Model Fe(II) Porphine (Å)

	X	*Y*	*Z*
Fe	0.0000	0.0000	0.0000
N2	2.0000	0.0000	0.0000
C7	2.8396	1.1001	0.0000
C15	4.2181	0.6745	0.0000
C23	2.4326	2.4326	0.0000
H27	5.0868	1.3161	0.0000
H35	3.1962	3.1962	0.0000

Fe–N2	2.0000 Å	N2–C7	1.384 Å	C7–C15	1.443 Å
C14–C15	1.349 Å	C7–C23	1.393 Å	C–H	1.080 Å
C6–N2–C7	105.3°	N2–C7–C23	125.7°	C8–C23–C7	124.0°
N2–C7–C15	110.2°	C7–C15–C14	107.2°		

culated spectra. The single excitations were generated by using nearly all of the π molecular orbitals, all of the d orbitals, the 4s and 4p "empty" orbitals of iron (giving rise, in our model, to Rydberg like transitions), and the highest occupied orbitals of σ symmetry. The resulting CI consists of about 200 configurations in each of the 8 irreducible representations of D_{2h}. The inclusion of additional configurations does affect the energies of states calculated above about 35 000 cm^{-1}, and therefore we do not report calculated states above about this value.

This model for calculating spectra has been tested on ionic transition-metal complexes where experimental spectra are available and was able to reproduce both the allowed transitions and the spin-forbidden transitions extremely well.[10] This is in part due to the high reliance of the INDO/CI methodology on atomic spectroscopy. We thus believe this model can predict the relative ordering of transition-metal spin states, of interest in this study.

The ability of this model to reproduce ligand $\pi \rightarrow \pi^*$ excitations is well established and its limitations are well understood.[6,20] For porphyrin-like systems the position of the Q band (visible) can be accurately calculated, though the Soret band is usually calculated 4000–5000 cm^{-1} too high.[21,22] The model is less well established for charge-transfer excitations within a transition-metal complex, but calculations on a related oxyheme complex[22] were successful in matching the experimental spectrum band for band. Although the experimental origins of the four lowest bands in oxyheme is not certain, the calculations indicated they are iron–oxygen in nature, and these bands do disappear upon deoxygenation. For the systems under study here, the location of iron to

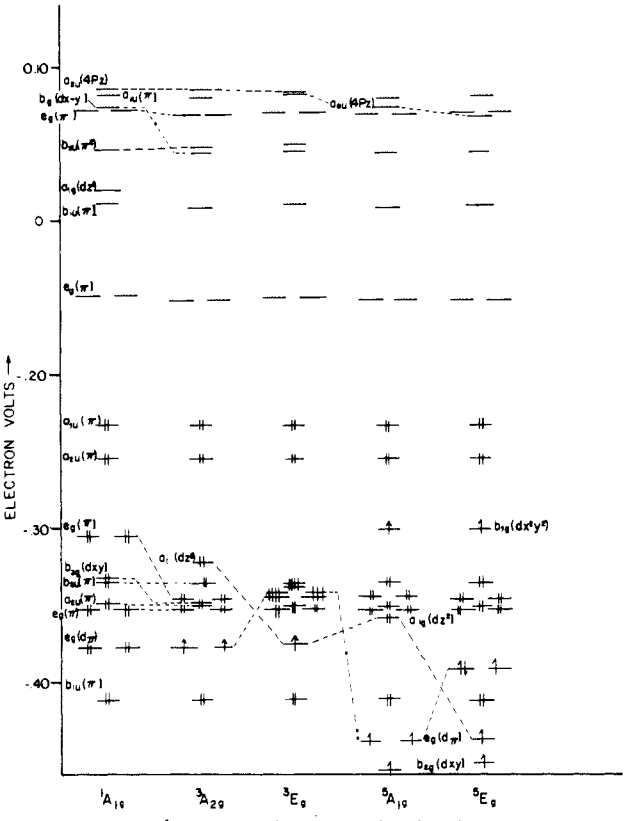

Figure 2. Molecular orbital eigenvalues for the highest occupied and lowest empty orbitals of the five lowest states of Fe(II)P. Note the break in scale between occupied and virtual.

porphyrin and porphyrin to iron charge-transer excitations is not well established experimentally, and different theoretical models give quite different estimates of where they should lie. We will discuss this later in the paper.

The geometry of Fe(II)P used for these calculations is given in Table I, and the atom labeling is given in Figure 1. The most significant difference between this structure and that given by Collman, Hoard, Kim, Lange, and Reed[4] for Fe(II) tetraphenylporphyrin (tetraphenylporphinato iron(II)) is the Fe–N bond length. We have chosen 2.00 Å as opposed to the experimentally reported value of 1.97 Å to better compare with the ab initio results of Rawlings et al.[23] and with those results of Sontum, Case, and Karplus[24] that were calculated at a distance of 2.01 Å. Since the Fe–N bond length determines the size of the central "hole" in porphyrin systems, this bond distance will affect the results obtained. We will also return to this point later.

There is an interesting technical point involved with the geometry chosen. Our original attempts at calculating this molecule were made on a geometry rotated 45° from that of Table I (nitrogen atoms on the *X*, *Y* axis). This rotated geometry led to symmetry breaking during the SCF, whereas the structure of Table I did not. We attribute this to very slight differences in numerical precision for the two structures. However, in spite of this symmetry breaking the final converged SCF energies were essentially the same. Clearly the ground-state structures we examined must lie close to a Hartree–Fock instability, as witnessed by the very many near-lying states we calculated.

3. Ground-State Calculations

The SCF and CI relative energies that we calculate for the lowest states of Fe(II)P are presented in Table II. The energies reported under "INDO/CI" are the lowest energies obtained for those states from any CI. Since there are two ^3E_g low-lying states

(20) See, for example: Ridley, J. E.; Zerner, M. C. *J. Mol. Spectrosc.* **1974**, *50*, 457.
(21) Edwards, W. D.; Zerner, M. C. *Int. J. Quantum Chem.* **1983**, *23*, 1407.
(22) Zerner, M. C.; Loew, G. H.; Herman, Z. S. *Int. J. Quantum Chem.* **1980**, *18*, 4kl.
(23) Rawlings, D. C.; Gouterman, M.; Davidson, E. R.; Feller, D. *Int. J. Quantum Chem.*, in press.
(24) Sontum, S. F.; Case, D. A.; Karplus, M. *J. Chem. Phys.* **1983**, *79*, 2881.

Table II. Low-Lying States of Fe(II) Porphine with ^3E_g States Taken as Reference and Relative Energies in eV[a]

state	configuration					INDO		ab initio[b]		
	x^2-y^2	z^2	xy	yz	xz	SCF	CI	SCF	CI	SCF[c]
$^5A_{1g}$	1	2	1	1	1	0.04	0.28	-1.40	-0.10	-1.53
^5E_g	1	1	1	1.5	1.5	0.17	0.39	-1.19	-0.83	-1.30
$^5B_{2g}$	1	1	2	1	1	1.37	0.63[d]	-1.05	0.09	-1.18
$^3A_{2g}$	0	2	2	1	1	-0.27	-0.03	-0.29	0.47	-0.32
$^3E_g(A)$	0	1	2	1.5	1.5	0.00	0.00	0.00	0.00	0.00
$^3B_{2g}$	0	1	1	2	2	0.16	0.39	0.51	0.20	0.56
$^3E_g(B)$	0	2	1	1.5	1.5	0.68	1.03[e]	1.42	1.12	1.43
$^1A_{1g}$	0	0	2	2	2	0.98	0.98	1.36	1.06	1.39
$^1A_{1g}$	0	2	0	2	2	3.50		5.89		
$^1B_{2g}$	0	1	1	2	2		1.76	1.58	1.66	
^1E_g	0	1	2	1.5	1.5		0.93		1.33	

[a] The lowest energies of each state are taken, regardless of which calculation yielded them; see text and footnotes *d* and *e*. [b] From ref 23, R(Fe-N) = 2.00 Å. [c] From ref 26, R(Fe-N) = 1.972 Å. [d] From a CI with ^5E_g as reference; see footnote *a*. [e] From a CI with $^3E_g(A)$ as reference; see footnote *a*.

Table III. Mulliken Population Analysis of Low-Lying Fe(II) Porphine States[a]

	$^1A_{1g}$	$^3A_{2g}$	$^3E_g(A)$	$^3E_g(B)$	$^5A_{1g}$	^5E_g
			Fe(II)			
d_{z^2}	0.075	1.885	0.985	1.855	1.900	0.997
$d_{x^2-y^2}$	0.456	0.487	0.470	0.547	1.231	1.219
d_{xy}	1.992	1.992	1.992	1.008	1.008	1.008
d_{xz}	1.973	1.011	1.494	1.488	1.018	1.502
Net d	6.468	6.386	6.363	6.386	6.175	6.228
4s	0.236	0.449	0.347	0.478	0.468	0.367
$4P_x = 4P_y$	0.167	0.163	0.164	0.188	0.189	0.162
$4P_z$	0.102	0.096	0.099	0.092	0.117	0.120
Net Q	0.832	0.742	0.790	0.719	0.863	0.908
Fe-N Wyberg	0.731	0.740	0.735	0.749	0.644	0.638
			N2			
net	-0.435	-0.430	-0.433	-0.422	-0.453	-0.455
π	1.526	1.535	1.529	1.532	1.531	1.527
			C7			
net	0.122	0.128	0.125	0.126	0.124	0.122
π	0.952	0.942	0.947	0.949	0.940	0.944
			C15			
net	-0.074	-0.073	-0.073	-0.073	-0.072	-0.073
π	1.014	1.010	1.012	1.012	1.010	1.011
			C23			
net	-0.061	-0.061	-0.061	-0.060	-0.062	-0.063
π	1.029	1.032	1.031	1.030	1.033	1.032

they are generated from the same CI to avoid problems of variational collapse. Mulliken populations at the SCF level for six of the more important states are reported in Table III. Figure 2 gives an orbital energy diagram for five of these states.

There is a great deal of experimental information available on this complex. There seems little question that the ground state is of intermediate spin, $S = 1$, and this is what we find. Our lowest quintet state is $^5A_{1g}$ and lies 0.3 ev above the ^3E_g state that we have used as the reference. the only experimental evidence for the position of this band is indirect; a study of the magnetic susceptibility suggests a value of about 0.6 ev.[33]

Our lowest calculated state is of $^3A_{2g}$ symmetry and is nearly degenerate with the reference ^3E_g state. This ordering, $^3A_{2g} < {}^3E_g$ is in agreement with most other theoretical work. For comparison, the larger CI results of Rohmer[25] yield the $^3A_{2g}$ below ^3E_g by some 0.27 ev. Rohmer's SCF energy for the $^3A_{2g}$ state is -2244.20 au, after CI on this state, -2244.48 au.

Obara and Kashiwaga[26] have made an estimate of the effect of a limited CI on their SCF results for the triplet manifold. Their ^3E_g state is preferentially lowered, reducing the splitting of 0.32 ev at the SCF level (see Table II) to 0.08 ev, with the $^3A_{2g}$ still lowest. This CI is limited only to states generated through d to d excitations. Obara and Kashiwaga's SCF energy for the $^3A_{2g}$ state is -2241.70 au.; after ligand field CI[26,27] they estimate an energy of -2241.71 au.

On the basis of MSX-α calculations, Sontum, Case, and Karplus suggest that the $^3A_{2g}$ state is 0.2 ev below the ^3E_g state.[24]

Table II also includes the most extensive ab initio calculations to date on the excited states of this model compound, those of Rawlings, Gouterman, Davidson, and Feller.[23] Although all the SCF calculations produce the $^3A_{2g}$ state below the ^3E_g state by about 0.3 ev, these are the only CI calculations to yield the ^3E_g state below the $^3A_{2g}$ state. The SCF energy of the $^3A_{2g}$ state obtained from these calculations is -2243.49 au. After CI, the energy they obtain for the $^3A_{2g}$ state is -2243.47 au. It should be noted that in order to use improved virtual orbitals for the configuration interaction, Rawlings et al. used orbitals from a $^6A_{1g}$ $[Fe(III)P]^+$ calculation for both their $^3A_{2g}$ and ^3E_g CI calculations.

The INDO/CI energies reported in Table II are from single excitations only from the corresponding SCF. Higher order correlation is assumed to be included in the experimental atomic parameters obtained from atomic spectroscopy. Though only single excitations are included in the CI, for these open-shell systems the reference-state energy is depressed by 0.25–0.65 ev, due to so-called "Brillouin theorem violating" configurations. These configurations have the form of an excitation of a single

(25) Rohmer, M.-M. *Chem. Phys. Lett.*, in press.
(26) Obara, S.; Kashiwaga, H. *J. Chem. Phys.* **1982**, *77*, 3155.
(27) Kashiwaga, H.; Takada, T.; Obara, S.; Migoshi, E.; Ohno, K. *Int. J. Quantum Chem.* **1978**, *14*, 13.

electron from a closed-shell orbital into a virtual orbital, accompanied by a spin flip of an open-shell electron. These types of configurations are formally related to the reference state by a double excitation and must be included in order to correctly describe the multiplet. They interact with the Hartree–Fock reference state through the Hamiltonian and hence seemingly violate Brillouin's theorem. This CI mixing preferentially depresses the two-determinant reference representation of the ^3E_g state over that of the one determinant $^3A_{2g}$. This is clear from our results, the CI results of Rawlings et al. and the smaller CI of Rohmer. The energy lowering of Rawlings et al., after a reasonably large CI, is of the same size as is our lowering, suggesting that correlation in the usual sense has not really been included. The large preferential lowering of the ^3E_g state is more likely an effect of the choice of $^6A_{1g}$ $[Fe(III)P]^+$ orbitals used in that CI and is similarly composed mostly of orbital relaxation and Brillouin theorem violating contributions.

The larger CI calculations of Rohmer, on the other hand, have depressed the SCF energy of both the $^3A_{2g}$ and ^3E_g states by about 7.6 ev and preserved the SCF order of $^3A_{2g} < {}^3E_g$. Although the CI lowering they obtain is some 10 times greater than that obtained by Rawlings et al., it is still a very small percentage of the total correlation energy available in such a large system with 120 valence electrons.

It is currently not possible to perform a CI large enough to include all the orbital relaxation necessary to describe each individual state, and the above results clearly demonstrate that for a limited CI one must choose starting orbitals carefully. For example, in our calculations generating all states from $^3A_{2g}$ orbitals led to a 0.30 ev split between $^3A_{2g}$ and ^3E_g, while generating each CI from SCF orbitals of the appropriate symmetry reduced this to 0.03 ev. In addition, the inclusion of porphyrin π orbitals into the CI seems to favor the $^3A_{2g}$ state. The reason for this is not clear.

Our calculations predict an intermediate spin $^3A_{2g}$ ground state and a close-lying ^3E_g state. This splitting is of the order of kT at room temperature, giving rise to the possibility of thermal mixing, as well as other complicating features that might alter either the multiplicity or the symmetry of the ground state.

Our complication concerns the geometry used in the calculation. It would be most desirable to optimize the geometry of each of the low-lying electronic states, but this is impractical. Our assumed structure for all electronic states is based on a D_{4h} idealization of the experimental structure of bis(piperidine)(tetraphenylporphinato)iron(II), which has a nearly planar porphyrin fragment and an Fe–N bond length of 1.97 Å.[4] This bond length was increased to 2.00 Å to be compatible to that used by Rawlings et al., who based their structure on bis(piperidineiron(II) tetraphenylporphyrin.[28] For comparison, the Fe–N bond length in 2-methylimidazole iron(II) tetraphenylporphyrin is 2.044 Å.[29] However, this compound has the iron atom 0.42 Å out of the plane of the four porphyrin nitrogen atoms and is clearly high spin.

Any lenghtening of the Fe–N bond, or out-of-plane motion of the iron atom, might be expected to favor a high-spin structure. At 2.00 Å our results favor an intermediate-spin ground state, and this would also be true for an Fe(II)–N bond length of 1.97 Å. Ab initio calculations at the SCF level favor high-spin configurations over lower spin, generally of the order of 1 ev per electron pair broken to generate the higher spin. The inclusion of correlation tends to repair this artificial advantage, as can be seen for example in Table II for the ab initio calculations of Rawlings et al. In their calculations, however, the amount of correlation they include does not reverse the order of spin multiplicities.

Sontum et al.[24] on the basis of MSX-α calculations estimate that the lowest state changes multiplicity from high spin at 2.01 Å to intermediate spin at 1.97 Å. A crossover point is estimated

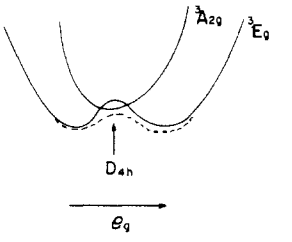

Figure 3. Schematic representation of the potential energy surfaces of the $^3A_{2g}$ and ^3E_g states long an e_g mode distorting the geometry from D_{4h}. Here we suggest that the ^3E_g could represent the global minimum even though the lower energy state with the D_{4h} geometry is calculated to be $^3A_{2g}$. The dashed line represents the potential that might be obtained from vibronic coupling of these two states long this mode.

at about 1.99 Å. Such a sensitive function of spin state vs. Fe(II)–N distance is not supported by the ab initio SCF calculations shown in Table II. Although different basis sets have been used, Rawlings et al. have performed their calculations at 2.00 Å, while Obara and Kashiwaga have performed theirs at 1.972 Å, and both predict a high-spin ground state. As discussed above, we believe that the triplet states in question, ^3E_g and $^3A_{2g}$, would lie lower in energy than the quintet states at both geometries.

The symmetry of the ground state may also depend on the geometry chosen. For the two close-lying ^3E_g and $^3A_{2g}$ states, we note that the former should undergo a distortion along an e_g symmetry vibrational mode, as depicted in Figure 3. We have made no attempt to optimize the geometries of these two states, but is possible that even if the $^3A_{2g}$ state lies lowest in energy at the D_{4h} symmetry, the ^3E_g state might represent a global minimum, as suggested in this figure. A further complication to this picture is the possible vibronic coupling between these two states, especially away from D_{4h} symmetry, for one of the components of $E_g \times E_g$ is A_{2g}. This coupling would lead to a very flat potential along this e_g mode and an electronic state that progresses from mostly $^3A_{2g}$ at C_{4h} symmetry to ^3E_g during an e_g vibration.

In addition to the geometric considerations just discussed, there is possible spin–orbit coupling between these two states via the X and Y components of this operator, also of e_g symmetry. This mixing is predicted to split the ground state into a ground-state singlet ($S_z = 0$) lying 70–90 cm^{-1} below the doublet ($S_z = \pm 1$),[30,31] and would blur the distinction between A_{2g} and E_g.

The experimental information on the ground-state symmetry of Fe(II)P is far from conclusive. The observed bond length of 1.972 Å strongly suggests intermediate spin when compared to other iron porphyrin systems with known spin.[4] Although the observed magnetic moments of about 4.40–4.75 μ_B[1] are closer to the 4-electron value of 4.90 μ_B than the 2-electron value of 2.83 BM, strong arguments based on the observed magnetic anisotropy favor a triplet state with a good deal of population in the empty $d_{x^2-y^2}$ orbital. This could be achieved via ligand-to-metal electron donating through orbitals involved in ligand-to-metal bonding.[4,30,33] These magnetic susceptibility measurements seem to show large zero-field splittings but suggest that the ground state is nondegenerate and at least 70 cm^{-1} below any excited state.[30,33]

The $^3A_{2g}$ ground state is also favored by the proton NMR studies,[31,32] which also suggest that the ground state is not orbitally degenerate and which indicate large π contact shifts most easily explained in terms of two unpaired electrons in the d_{xz} and d_{yz} orbitals. However, again we note that during the lifetime of the NMR experiment both the d_{xz} and d_{yz} orbitals would have unpaired spin density even in the ^3E_g state, though, in that case, the magnitude of the shifts would suggest only one unpaired electron

(28) Randonovitch, L. J.; Bloom, A.; Hoard, J. L. *J. Am. Chem. Soc.* **1972**, *94*, 2073. (1972).
(29) Jameson, G. B.; Malinaro, F. S.; Ibers, J. A.; Collman, J. P.; Brauman, J. I.; Rose, E.; Suslish, K. S. *J. Am. Chem. Soc.* **1978**, *100*, 6769.
(30) Lang, G.; Spartalian, K.; Reed, C. A.; Collman, J. P. *J. Chem. Phys.* **1978**, *69*, 5424.
(31) Goff, H.; LMar, G. N.; Reed, C. A. *J. Am. Chem. Soc.* **1977**, *99*, 3641.
(32) Mispelter, J.; Manenteau, M.; Lhoste, J. M. *J. Chem. Phys.* **1980**, *72*, 1003.
(33) Boyd, P. P. W.; Buckingham, D. A.; McMeeking, R. F.; Mitra, S. *Inorg. Chem.* **1979**, *18*, 3585.

rather than two. Furthermore, if the ^3E_g state was the ground state, the magnetic anisotropy would be expected to have $X(z) > X(x) = X(y)$, is disagreement with the experimental findings that $X(z) < X(x) = X(y)$.[32,33]

Resonance Raman studies, on the other hand, are most readily consistent with a ^3E_g ground state.[34] The argument here centers on the similarity of the observed frequencies to those obtained in low-spin Fe(III) porphyrin complexes which are clearly ^2E_g and which have three d_π (d_{xz} and d_{yz}) electrons.

The observed Mössbauer quadrupole splittings of 1.51 mm/s[4] to 1.60 mm/s[35] seems to support neither the $^3A_{2g}$ or ^3E_g states. Crystal field calculations yield −2.7 mm/s for the $^3A_{2g}$ state,[30] while the ab initio calculations of Rawlings et al. yield values of −0.75 mm/s for the $^3A_{2g}$ state and +0.74 mm/s for the ^3E_g state. Obawa and Kashiwaga have tried to explain the observed splitting by invoking configurational mixing of the two lowest ^3E_g states in Table II. They conclude that a 70%–30% mix these two states should yield the correct Mossbauer quadrupole splitting. However ab initio CI calculations[23,25] as well as INDO calculations reported here do not significantly mix these two states.

The ab initio calculations, however, show very little anisotropy in the orbital occupation of the 4p orbitals, a consideration in the calculations of the quadrupole splitting pointed out by Sontum et al.[24] Their calculations show a much greater 4p occupation and a much greater anisotropy than do the ab initio calculations. Their d orbital contributions to the quadrupole splitting in the $^3A_{2g}$ state of −2.4 mm/s is reversed by a p orbital contribution of +2.9 mm/s to yield a final value of +0.5 mm/s.

Using a Sternheimer correction of 0.92 and a nuclear quadrupole moment of 0.15 as suggested by Lauer et al.,[36] we calculate a quadrupole splitting of −0.78 mm/s for the $^3A_{2g}$ state and +1.77 mm/s for the ^3E_g state. The value for the $^3A_{2g}$ state is reasonably close to that of Rawlings et al.,[23] who used the same factors. Our value of 1.77 mm/s for the ^3E_g state is close enough to the observed values of 1.51–1.60 mm/s to strongly suggest that it is the ^3E_g state that is observed. Mixing of this state with the $^3A_{2g}$ state either through vibronic or spin–orbit coupling might be expected to lower this value, in better agreement with experiment. Thermal mixing, however, seems unlikely as the Mössbauer quadrupole splitting, at least for Fe(II)TPP, appears temperature independent from 4 to 300 K.[30] Our value of +1.77 mm/s lies between 2.66 mm/s obtained by Obara and Kashiwaga and 0.74 mm/s obtained by Rawlings et al. It is larger than the latter value mostly because of the greater $d_{x^2-y^2}$ population (0.47*e* vs. 0.26*e*, Table III) obtained in our calculation. The other d orbital populations are nearly identical in the two studies. Although our 4p orbital anisotropy is very similar to that calculated by Sontum et al. (see Mulliken populations in Table III), we find that this anisotropy has little effect on the ca ulated quadrupole splittings of either state.

Finally, we note that an electron density deformation map has been observed by Coppens and Li on Fe(II) phthalocyanine (Fe(II)Pc) that has been interpreted as most compatible with a ^3E_g ground state.[37] Although the electron deformation maps calculated by Rohmer[25] show that both ^3E_g and $^3A_{2g}$ states have similar maps in the porphyrin plane, perpendicular to this plane the $^3A_{2g}$ state with two d_{z^2} electrons has considerably more electron extension above the iron atom than does the ^3E_g state with only one d_{z^2} electron. This is what is observed and what has been inferred from a d orbital population calculated from experimentally determined multipole parameters.[37] We note, however, two provisos. The large anisotropy of the 4p populations suggested by Sontum et al. and confirmed in our calculations would also lead to an apparent depopultion of the d_{z^2} orbital, making the electron deformation maps of $^3A_{2g}$ more like the ^3E_g maps. This anisotropy in 4p orbital population is not reflected in Rohmer's calculation and thus does not appear in her theoretically calculated maps. However, Li and Coppens[37] argue that even a large 4p anisotropy might not be large enough to yield the experimental results. Nevertheless, in the absence of these 4p contributions, Li and Coppens "experimental" populations in the $d_{x^2-y^2}$ orbital of 0.75*e* is considerably higher than the value of 0.47*e* we obtain, while their d_{z^2} value of 0.88*e* is somewhat lower than our value of 0.99*d*, and their d_π value of 2.13*e* is closer to our $^3A_{2g}$ state (2.02*e*) than our ^3E_g state (2.99*e*)!

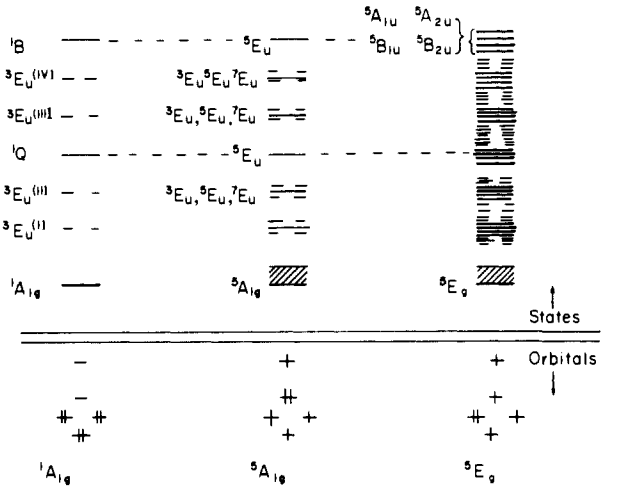

Figure 4. Schematic representation of the coupling of a quintet Fe(II) ion of $^5A_{1g}$ or ^5E_g symmetry with the low-lying singlet and triplet states of porphyrins. Only states of E_u symmetry are shown. The location of ^3E_u(IV) state with respect to the soret band is uncertain and is most often calculated nearly degenerate with the ^1B.

The second proviso is a more pragmatic one. Fe(II)Pc with an Fe–N bond length of 1.927 Å is not Fe(II)P, which has a considerably longer bond length of 1.972–2.01 Å. If it were not for this crucial difference, we would consider the electron density deformation map as the most convincing argument for a ^3E_g ground state.

4. UV–Visible Spectroscopy

The spectra of all porphyrin complexes are dominated by the $\pi \rightarrow \pi^*$ transitions. There is a relatively weak band (Q) in the visible, often with broad vibrational structure, and an intense "soret" (B) in the near UV. These bands have been most successfully described by a four-orbital model, shown in Figure 2, that mixes configurations generated from $a_{1l}(\pi) \rightarrow e_g(\pi^*)$ and $a_{2u}(\pi) \rightarrow e_g(\pi^*)$ frontier orbital excitations. These two excited configurations are of E_u symmetry and are predicted to have nearly equal intensity. However, they will strongly interact, leaving the lower band (Q) weak and the higher one (B) strong. This situation is described on the left-hand side of Figure 4 and the right-hand sides of Figures 5 and 6 and is referred to as the four-orbital model.[38,39,12] The two triplets from these two excitations do not mix directly with each other and are believed to lie below the Q band. Two other triplets, arising from excitations out of the orbitals of $b_{2u}(\pi)$ and $a_{2u}(\pi)$ symmetry into the LUMO $e_g(\pi^*)$ are shown in Figure 3. The higher of these triplets is calculated to be nearly degenerate with the Soret and is best depicted in the $^1A_{1g}$ case of Figure 3, where the spin of the central metal has no perturbing influence on the low-lying porphyrin π–π^* bands.

The ground state of simple porphyrin is $^1A_{1g}$. The introduction of a paramagnetic metal atom, for example, of $^5A_{1g}$ symmetry as shown in Figure 4, causes spin coupling with the porphyrin π states. The ground state in this example then becomes quintet, as are the Q and B excited states. The four triplet states of simple porphyrin shown in Figure 4 will couple with the quintet metal atom to give states of triplet, quintet, and septet multiplicities. Excitations from the quintet ground state to the quintet component of this triplet are now spin allowed and are called trip-quintets.[11]

(34) Kitagawa, T.; Teraoka, J. *Chem. Phys. Lett.* **1979**, *63*, 443.
(35) Dolphin, D.; Sams, J. R.; Tsin, T. B.; Wong, K. L. *J. Am. Chem. Soc.* **1976**, *98*, 6970.
(36) Lauer, S.; Marathe, V.; Trantwers, A. *Phys. Rev. A* **1979**, *19*, 1852.
(37) Coppens, P.; Li, L. *J. Chem. Phys.* **1984**, *81*, 1983.
(38) Gouterman, M. *J. Mol. Spectroc.* **1961**, *6*, 138.
(39) Weiss, C.; Kobayashi, H. Gouterman, M. *J. Mol. Spectrosc.* **1965**, *16*, 415.

Table IV. Calculated d → d* Spectra from $^3E_g(d_{z^2}d^3_\pi d^2_{xy})$ in 1000 cm^{-1}

state	configuration				energy	
	π	xy	z^2	x^2-y^2	INDO/CI	ref 23
$^3E_g(A)$	3	2	1	0	0.0	0.0
$^3A_{2g}(d_\pi \rightarrow d_{z^2})$	2	2	2	0	-0.2	3.8
$^3B_{2g}(d_{xy} \rightarrow d_\pi)$	4	1	1	0	1.8	1.4
$^3E_g(d_{xy} + d_{z^2})$	3	1	2	0	9.3	9.0
$^3A_{2g}(d_{xy}, d_{z^2} \rightarrow d_\pi, d_{x^2-y^2})$	4	1	0	1	16.5[a]	15.9
$^3E_g(d_{xy} \rightarrow d_{x^2-y^2})$	3	1	1	1	19.5[b]	17.3
$^3B_{1g}(d_{xy}, d_{xy} \rightarrow d_\pi, d_{x^2-y^2})$	4	0	1	1		17.8
$^3B_{1g}(d_{xy}, d_\pi \rightarrow d_{z^2}, d_{x^2-y^2})$	2	1	2	1	19.0[c]	19.7-21.6
$^3B_{2g}(d_\pi \rightarrow d_{x^2-y^2})$	2	2	1	1	19.4	20.2
$^3E_g(d_\pi, d_\pi \rightarrow d_{z^2}, d_{x^2-y^2})$	1	2	2	1	24.4[b]	
$^5A_{1g}(d_\pi, d_{xy} \rightarrow d_{z^2}, d_{x^2-y^2})$	2	1	2	1	2.4, 2.3	-0.8
$^5E_g(d_{xy} \rightarrow d_{x^2-y^2})$	3	1	1	1	3.2, 6.8	-6.7
$^5B_{2g}(d_\pi \rightarrow d_{x^2-y^2})$	2	2	1	1	5.1, 8.2	0.7
$^5B_{1g}(d_\pi, d_{xy} \rightarrow d_{x^2-y^2}, d_{x^2-y^2})$	2	1	1	2	21.0	17.7
$^1A_{1g}(d_{z^2} \rightarrow d_\pi)$	4	2	0	0	7.9	8.5
^1E_g	3	2	1	0	7.4	10.7
$^1B_{2g}(d_{xy} \rightarrow d_\pi)$	4	1	1	0	14.2	17.7
$^1A_{1g}(d_\pi \rightarrow d_{z^2})$	2	2	2	0		13.4
$^1B_{2g}(d_\pi \rightarrow d_{z^2})$	2	2	2	0		14.3
$^1B_{1g}(d_\pi \rightarrow d_{z^2})$	2	2	2	0		18.7
$^1A_{2g}(d_{xy}, d_{z^2} \rightarrow d_\pi, d_{x^2-y^2})$	4	1	0	1	28.5	24.8
$^1E_g(d_{xy} \rightarrow d_{z^2})$	3	1	2	0		20.9
$^1E_g(d_{xy} \rightarrow d_{x^2-y^2})$	3	1	1	1		26.4
$^1E_g(d_{z^2} \rightarrow d_{x^2-y^2})$	3	2	0	1	36.3	

[a] From $^3B_{2g}$ CI. [b] From $^5A_{1g}$ CI. [c] From $^3A_{2g}$ CI.

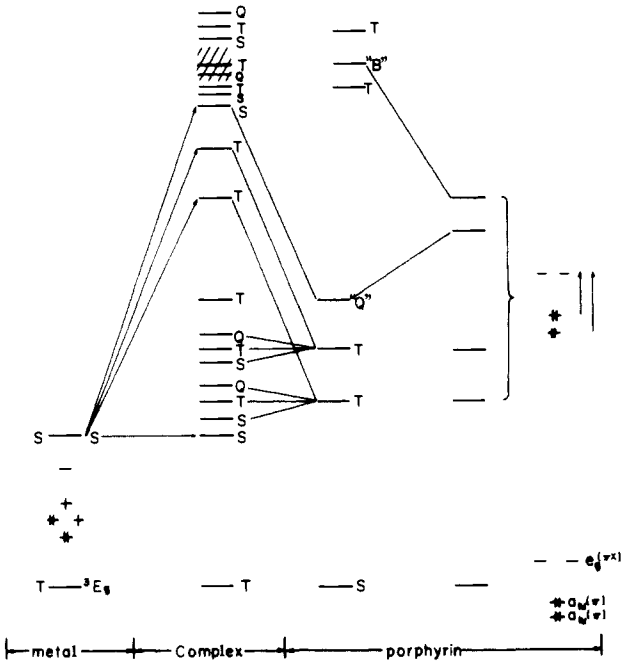

Figure 5. Schematic coupling of the low-lying states of porphyrins with a triplet metal ion. This situation lies closest to a ^3E_gFe(II) state, a situation in which each line of the complex in the diagram represents four states, $E_uE_g = A_{1u} + A_{2u} + B_{1u} + B_{2u}$.

Should the central metal atom also have a spatially degenerate configuration, for example, ^5E_g as shown in Figure 4, each of the triplet E_u states will split into four components of $^5A_{1u}$, $^5A_{2u}$, $^5B_{1u}$, and $^5B_{2u}$ symmetry. A simple porphyrin π triplet has now split into 12 states, even ignoring spin degeneracies.

In addition to the coupling just described, the metal atom itself may have different multiplicities. A triplet metal atom, such as the ^3E_g $(d^2_{xy}, d^2_{xz}, d_{yz}, d_{z^2}) = {}^3E_g(A)$ shown in Figure 5, has a higher lying $^1E_g(A)$ state as well as $^3E_g(A)$. Both the singlet and the triplet of the transition-metal couple with the singlet and triplet singly excited porphyrin states, yielding $2^4 = 16$ states. The triplet metal atom couples with the singlet porphyrin to yield a triplet (sing-triplet) and with the triplet porphyrin to yield a quintet, triplet, and a singlet (trip-triplets) as described in Figure 4. The singlet metal state also couples with the singlet and triplet porphyrin states, giving rise to a singlet (sing-singlet) and triplet (sing-triplet) as presented in Figure 5.

The ^5E_g $(d_{xy}, d^2_{xz}, d_{yz}, d_{z^2}, d_{x^2-y^2})$ situation of Figure 6 is, of course, more complicated, for the four open d shells generate a quintet, 3 triplets, and 2 singlets. Components of two of these sing-triplets and trip-triplets are predicted to lie near or below the B band.

In the above description we have treated each transition-metal configuration as if it generated a somewhat separate species from others. In reality, the low-lying available states are generated from the union of all such pictures (Figures 4 and 5) for each of the states, as suggested in Table II. This represents a large number of low-lying states. Recalling that in the case of an orbitally degenerate metal ion E_g state, we see that each line of these figures represents four orbitally nondegenerate states; the subsequent tables of calculated states would be nearly impossible to understand without recourse to Figures 5 and 6.

In the above we have focused attention on the $\pi \rightarrow \pi^*$ spectra calculated from any given d electron configuration of the central metal atom. The various metal configurations are generated by d → d transitions. We present our calculated d → d transitions in Table IV using the $^3E_g(A)$ state as the reference state. In this picture our $^3A_{2g}$ $(d_\pi \rightarrow d_{z^2}) = {}^3A_{2g}$ $(d^2_{xy}, d_{xz}, d_{yz}, d^2_{z^2})$ is a deexcitation. Our calculated excitation energies for the triplet states are remarkably close to those of Rawlings et al.[23] The low-lying singlet states, where they can be compared, are also in good agreement, whereas all our quintet states are calculated about 5000 cm^{-1} higher than the ab initio results. As mentioned, the lower energy of the quintet states calculated by the ab initio methods are probably a consequence of the SCF procedure that prefers open-shell structures (Table II). Given this rationale, the good agreement we obtain with the ab initio calculations for the singlet (Table II and Table IV) is remarkable. Another interesting aspect of this comparison is that the INDO calculations suggest that the $^5A_{1g}$ state remains the lowest quintet even after CI, whereas the ab initio study suggests that the ^5E_g state should lie lowest.

Assuming the lowest lying metal atom configuration of each multiplicty, we present the predicted UV–visible absorption spectra that we calculated in Tables V–IX. These are the results of SCF calculations on each of those states and CI's generated by using

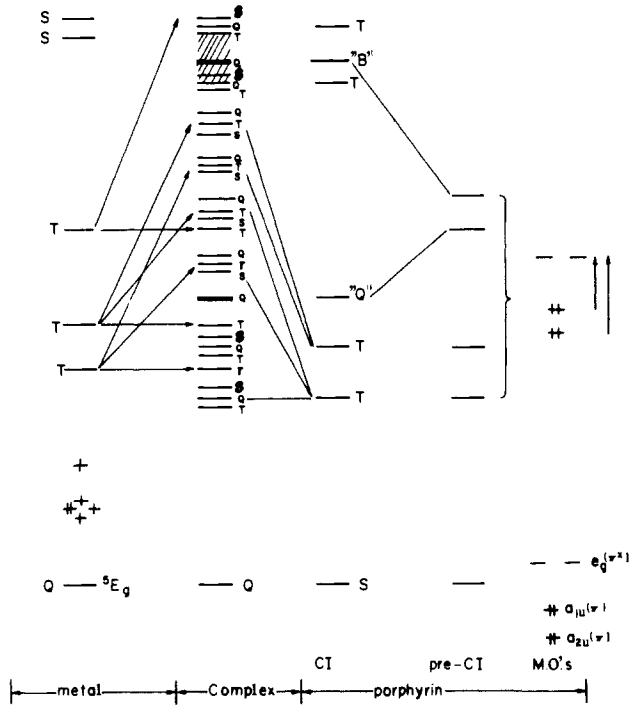

Figure 6. Shcematic coupling of the low-lying states of porphyrin with a quintet metal ion. This situation lies closest to a ^5E_g Fe(II) state, a situation in which each line of the complex represents four states, $E_u \times E_g = A_{1u} + A_{2u} + B_{1u} + B_{2u}$; see text.

Table V. Calculated Spectrum of $^1A_{1g}$ Ground-State Fe(II) Porphine (1000 cm^{-1})

state	energy	comments	
$^3B_{2g}$	-2.9	$b_{2g}(d_{xy}) \rightarrow a_{1g}(d_{z^2})$	
^1E_g	-0.5	$e_g(d_\pi) \rightarrow a_{1g}(d_{z^2})$	
$^1B_{2g}$	6.3	$b_{2g}(d_{xy}) \rightarrow a_{1g}(d_{z^2})$	
^3E_u	11.1	$a_{1u}(\pi) \rightarrow e_g(\pi^*)$	
^3E_u	15.3	$a_{2u}(\pi) \rightarrow e_g(\pi^*)$	
^1E_u	16.3 [0.126]	$\pi \rightarrow \pi^*$	Q
^3E_g	18.5	$e_g(\pi) \rightarrow a_{1g}(d_{z^2})$	CT
$^1A_{2g}$	20.6	$a_{1g}(d_{z^2}) \rightarrow b_g(d_{x^2-y^2})$	
^1E_g	28.4	$e_g(d_\pi) \rightarrow b_{1g}(d_{x^2-y^2})$	
^3E_u[b]	30.1	$\pi \rightarrow \pi^*$	
^1E_u	30.3 [6.10]	$\pi \rightarrow \pi^*$	B
^1E_u	34.8 [0.18]	$\pi \rightarrow \pi^*$	N

[a] Only singlet excitations beyond this energy are shown, except for the third $\pi \rightarrow \pi^*$ ^3E_u. [b] Only strongly allowed transitions shown beyond this state; see text.

Table VI. Calculated Triplet Spectrum of $^3A_{2g}$ Ground-State Fe(II) Porphine (1000 cm^{-1})

state	energy (OSC)	comments		
^3E_g	2.4	81% $a_{1g}(d_{z^2}) \rightarrow e_g(d_\pi)$ + 19% $b_{2g}(d_{xy}) + e_g(d_\pi)$		
^3E_u	8.5 (0.012)	$a_{1u}(\pi) \rightarrow e_g(\pi^*)$	trip-trip	(1)
^3E_g	11.0	78% $b_{2g}(xy) + e_g(d_\pi)$ + 19% $a_{1g}(d_{z^2}) + e_g(d_\pi)$		
^3E_u	13.2 [0.002]	$a_{2u}(\pi) + e_g(\pi^*)$	trip-trip	(1)
^3E_u	15.9 [0.115]	$a_{2u}(\pi)$, $a_{1u}(\pi) \rightarrow e_g(\pi^*)$	Q	(1)
^3E_u	19.0 [0.001]	$a_{1u}(\pi) \rightarrow e_g(\pi^*)$	sing-trip	(1)
$^3B_{1g}$[a]	19.2	$b_{2g}(xy) \rightarrow b_{1g}(d_{x^2-y^2})$		
^3E_u	23.7 [0.015]	$a_{2u}(\pi) \rightarrow e_g(\pi^*)$	sing-trip	(1)
^3E_u	24.6 [0.001]	$\pi \rightarrow \pi^*$	trip-trip	(2)
^3E_u	29.2 [4.854]	$a_{1u}(\pi)$, $a_{2u}(\pi) \rightarrow e_g(\pi^*)$	B	(1)
^3E_u	30.8 [0.089]	$\pi \rightarrow \pi^*$	trip-trip	(2)
^3E_u	32.0 [0.008]	$\pi \rightarrow \pi^*$		(2)
^3E_u	34.8 [0.169]	$\pi \rightarrow \pi^*$	N	(2)
$^3B_{1u}$	34.8 [0.103]	$a_{1g}(d_{z^2}) \rightarrow a_{2u}(4P_z)$	Rydberg	

[a] Only allowed transition are shown above 20000 cm^{-1}.

the appropriate SCF orbitals of the reference state. The intensities are dominated by single excitations among the valence orbitals.

Table VII. Calculated Triplet Spectrum of ^3E_g Ground-State Fe(II) Porphine (1000 cm^{-1})

state	energy	comments		
$^3A_{2g}$	-0.2	$e_g(d_\pi) \rightarrow a_{1g}(d_{z^2})$		
$^3B_{2g}$	1.8	$b_{2g}(d_{xy}) \rightarrow e_g(d_\pi)$		
^1E_g	7.4	"spin flip"	sing-sing	
^3E_g	9.3	$b_{2g}(d_{xy}) \rightarrow a_{1g}(d_{z^2})$		
$^3A_{1u}$, $^3A_{2u}$	9.1 [1.3 × 10^{-3}], 11.0 [1 × 10^{-4}]	$a_{1u}(\pi) \rightarrow e_g(\pi^*)$	trip-trip	(1)
$^3B_{1u}$, $^3B_{2u}$	11.2 [0.0000], 11.3 [0.0000]			
$^3A_{2u}$, $^3A_{1u}$	14.4 [3 × 10^{-4}], 15.5 [1.6 × 10^{-3}]	$a_{2u}(\pi) \rightarrow e_g(\pi^*)$	trip-trip	(1)
$^3B_{1u}$, $^3B_{2u}$	15.8 [0.0000], 15.8 [0.0000]			
$^3A_{1u}$, $^3A_{2u}$	16.9 [0.012], 17.7 [0.016]			(1)
$^3B_{1u}$, $^3B_{2u}$	18.0 [0.003], 18.0 [0.028]	$\pi \rightarrow \pi^*$ [0.120]	Q	
$^3A_{1u}$, $^3B_{2u}$	18.1 [0.025], 18.1 [0.005]	$a_{1u}(\pi) \rightarrow e_g(\pi^*)$	sing-trip	(1)
$^3B_{1u}$, $^3A_{2u}$	18.1 [0.028], 18.2 [0.004]			

Table VIII. Calculated Spectrum of $^5A_{1g}$ Ground-State Fe(II) Porphine (1000 cm^{-1})

state	energy	comments	
$^3A_{2g}$	-2.3	$b_{1g}(d_{x^2-y^2}) \rightarrow b_{2g}(d_{xy})$	
^3E_g	4.1	$b_{1g}(d_{x^2-y^2}) \rightarrow e_g(d_\pi)$	
^5E_g	4.5	$a_{1g}(d_{z^2}) \rightarrow e_g(d_\pi)$	
$^5B_{2g}$	5.9	$a_{1g}(d_{z^2}) \rightarrow b_{2g}(d_{xy})$	
^3E_u	9.1		
^5E_u	9.3 (6.0 × 10^{-4})	$a_{1u}(\pi) \rightarrow e_g(\pi^*)$	trip-quint
^7E_u	9.6		
$^3A_{1g}$	12.8	spin flip	sing-trip
^3E_u	14.0		
^5E_u	14.1 (1.0 × 10^{-4})	$a_{2u}(\pi) \rightarrow e_g(\pi^*)$	trip-quint
^7E_u	14.3		
^5E_u	15.9 (0.120)	$a_{1u}(\pi)$, $a_{2u}(\pi) \rightarrow e_g(\pi)^*$	Q
$^3B_{2g}$	17.1	$a_{1g}(d_{z^2}) \rightarrow b_{2g}(d_{xy})$	
$^3A_{1g}$	18.6	spin flip	sing-trip
$^3A_{1g}$[a]	18.7	spin flip	sing-trip
^5E_u	22.6 (1.0 × 10^{-4})	$a_{1u}(\pi) \rightarrow e_g(\pi^*)$	trip-trip
^5E_u	27.3 (0.056)	$a_{2u}(\pi) \rightarrow e_g(\pi^*)$	trip-trip
^5E_u	27.6 (0.182)	$\pi \rightarrow \pi^*$	trip-quint
^5E_u	28.2 (0.178)	$a_{1u}(\pi) \rightarrow e_g(\pi^*)$	trip-trip
^5E_u	28.8 (0.228)	$a_{1u}(\pi) \rightarrow e_g(\pi)^*$	trip-trip
^5E_u	29.6 (4.160)	$a_{1u}(\pi)$, $a_{2u}(\pi) \rightarrow e_g(\pi^*)$	B
^5E_u	32.7 (0.363)	$\pi \rightarrow \pi^*$	N
^5E_u	33.2 (0.056)	$\pi \rightarrow \pi^*$	mixed

[a] Only allowed transitions above this energy are reported.

Table V presents the results for a $^1A_{1g}$ ground state, the simple situation shown on the right side of Figure 4 and in the middle of Figure 5 and 6. The triplets are shown for reference though they are spin forbidden from the ground state. Observed Q bands for such systems are generally around 16000 cm^{-1}.[12,40] The Soret band is generally observed at about 24000 cm^{-1}; our calculated values are 5000–6000 cm^{-1} too high for all of these systems.[21,22] Two ^3E_u states are calculated below the $^1E_u(Q)$ state. The next two ^3E_u states (only one shown in Table V) are calculated to lie near the $^1E_u(B)$ band. Because further CI would preferentially depress the singlet B state more than the triplets, the actual location of these two triplet states relative to the B band must be considered uncertain. The calculated spectra of the $^3A_{2g}$ state appears in Table VI and that of the ^3E_g state in Table VII. The two trip-triplets calculated at 8500 and 13200 cm^{-1} from the $^3A_{2g}$ state and at about 10000 and 15000 cm^{-1} from the ^3E_g state are allowed and might be compared to two observed peaks at about 12500 and 15000 cm^{-1}.[10] Although the intensity from the $^3A_{2g}$ ground state for these two trip-triplets transitions is greater (about 10% of the Q band), the predicted energy from the ^3E_g seems in

(40) Edwards, L.; Dolphin, D. H.; Gouterman, M. *J. Mol. Spectroc.* **1970**, *35*, 90.

Table IX. Calculated Quintet Spectrum of ^5E_g

state	energy	comments	
$^5A_{1g}$	0.8	$e_g(d_\pi) \rightarrow a_{1g}(d_{z^2})$	
$^5B_{2g}$	1.9	$e_g(d_\pi) \rightarrow b_{2g}(d_{xy})$	
$^5B_{2u}$, $^5A_{2u}$	8.5 (0.0014), 10.2 (0)	$a_{1u}(\pi) \rightarrow e_g(\pi^*)$	trip-quint (1)
$^5A_{1u}$, $^5B_{1u}$	10.2 (0) 10.2 (0)		
$^5A_{1u}$, $^5B_{2u}$	13.3 (1×10^{-4}), 14.7 (7×10^{-4})	$a_{2u}(\pi) \rightarrow e_g(\pi^*)$	trip-quint (1)
$^5B_{1u}$, $^5A_{2u}$	14.8 (0), 14.8 (0)		
$^5B_{2u}$, $^5A_{1u}$	16.0 (0.0403), 16.2 (0.0227)	$a_{1u}(\pi)$, $a_{2u}(\pi) \rightarrow e_g(\pi^*)$	Q (0.131) (1)
$^5B_{1u}$, $^5A_{2u}$	16.4 (0.0346), 16.5 (0.0333)		
$^5B_{1g}$	17.8	$e_g(d_\pi) \rightarrow b_{1g}(d_{x^2-y^2})$	
^5E_g	21.7	$e_g(d_\pi) \rightarrow e_g(\pi^*)$	TX
$^5B_{2u}$, $^5A_{2u}$	23.4 (0.0013), 23.6 (0)	$a_{1u}(\pi) \rightarrow e_g(\pi^*)$	trip-trip (1)
$^5B_{1u}$, $^5A_{1u}$	23.6 (0), 23.8 (0)		
$^5B_{2u}$, $^5A_{1u}$	24.7 (0.0075), 26.5 (0.0762)	$a_{1u}(\pi)$, $a_{2u}(\pi) \rightarrow e_g(\pi^*)$	trip-trip (1)
$^5B_{1u}$, $^5A_{2u}$	26.7 (0), 26.7 (0)	$b_{2u}(\pi) \rightarrow e_g(\pi^*)$	Trip-Quint
$^5A_{1u}$, $^5B_{1u}$	27.2 (0.3135), 27.6 (4×10^{-4})	$a_{2u}(\pi) \rightarrow e_g(\pi^*)$	trip-trip (1)
$^5A_{2u}$, $^5B_{2u}$	28.2 (2×10^{-4}), 28.3 (0)		
$^5A_{1u}$, $^5B_{1u}$	28.2 (0.054), 28.3 (1.-4)	$\pi \rightarrow \pi^*$	mixed
$^5B_{2u}$, $^5A_{2u}$	29.0 (0.009), 29.0 (0)		trip-trip
$^5A_{1u}$, $^5B_{2u}$	28.9 (0.183), 29.7 (0.278)	$\pi \rightarrow \pi^*$	trip-quint
$^5B_{1u}$, $^5A_{2u}$	30.1 (0.016), 30.2 (0.021)		
$^5A_{1u}$, $^5B_{2u}$	30.3 (0.019), 31.1 (0.018)	$\pi \rightarrow \pi^*$	trip-quint
$^5A_{2u}$, $^5B_{1u}$	31.2 (0.001), 31.2 (0.000)		
$^5B_{1u}$, $^5B_{2u}$	30.2 (1.274), 30.2 (0.873)	$a_{1u}(\pi)$, $a_{2u}(\pi) \rightarrow e_g(\pi^*)$	B (3.925)
$^5A_{2u}$, $^5A_{1u}$	30.3 (1.292), 30.6 (0.486)	$a_{1u}(\pi)$, $a_{2u}(\pi) \rightarrow e_g(\pi^*)$	
$^5B_{1u}$, $^5A_{1u}$	33.3 (0.016), 33.4 (0.035)	$b_{2u}(\pi)$, $a_{2u}(\pi) \rightarrow e_g n\pi^*)$	N (0.213)
$^5B_{2u}$, $^5A_{2u}$	34.1 (0.046), 34.7 (0.116)	$b_{2u}(\pi)$, $a_{2u}(\pi) \rightarrow e_g(\pi^*)$	

better agreement with experiment if the assignment of the trip-triplets corresponds to these observed transitions.

The calculated transitions of Table VII are best understood by comparison with Figure 5. We note that the Q band is predicted to be broadened by the presence of the close-lying sing-triplet. Transitions from 16 900 to 18 200 cm^{-1} all have calculated oscillator strengths adding up to $f = 0.120$, as compared with a single Q transition with the same oscillator strength calculated at 15 400 cm^{-1} from the $^3A_{2g}$ reference ground state. In a similar fashion, the B band is calculated to be broadened and at slightly higher energy when estimated from the ^3E_g reference state.

The calculated spectra of the $^5A_{1g}$ and ^5E_g (see Figures 4 and 6) are tabulated in Tables VIII and IX. In Table VIII are included the triplet, quintet, and septet spin components of the two lowest lying trip-quintets. In both cases the order is triplet < quintet < septet. Antiferromagnetic coupling is preferred over ferromagnetic coupling. The reason for this is not clear, but this order has also been calculated by Rawlings et al.[23] The spin splitting in both trip-quintets is small, less than 500 cm^{-1} in both cases.

In Table IX only the quintets are reported. Each porphyrin E_u state is again split into $A_{1u} + A_{2u} + B_{1u} + B_{2u}$ allowed components. The trip-quintets are split by some 1500 cm^{-1}, but the Q band and the B band are predicted to be split by about 500 cm^{-1}. The $\pi \rightarrow \pi^*$ spectra predicted from the $^5A_{1g}$ and ^5E_g reference states are nearly identical.

In Table X are tabulated the calculated results for all low-lying charge-transfer excitations from Fe to porphyrin and from porphyrin to Fe. A sharp delineation of such excitations in a molecular orbital configuration interaction calculation is difficult to make, but we have separated those excitations that transfer half an electron or more.

In general, we find that electron transfer from metal to porphyrin, resulting in $Fe(III)^+P^-$, lie lower in energy than those involving transfer from porphyrin to Fe, resulting in $Fe(I)^-P^+$. Transitions of the former type are all $d \rightarrow e_g(\pi^*)$, where $e_g(\pi^*)$ is the LUMO. Our lowest lying excitations of this type is of ^5E_g symmetry predicted at 24 800 cm^{-1}, or between the calculated Q and B bands.

Somewhat surprising is the calculation of the lowest lying $Fe(I)^-P^+$ state at 26 400 cm^{-1} involving $e_g(\pi) \rightarrow a_{1g}$ (dz_2). This $e_g(\pi)$ orbital lies more than 0.1 ev below the HOMO $a_{1u}(\pi)$ MO (Figure 2), but the resultant state of ^3E_g symmetry is considerably lowered through configurational mixing.

For comparisons, all of our quintet $Fe(III)^+P^-$ charge-transfer states lie about 10 000 cm^{-1} above those reported by Rawlings et al.[23] Sontum et al.[24] have made estimates of some of these charge-transfer excitations from their MSX-α calculations, predicting charge-transfer states of both metal → ligand and ligand → metal at lower energies than we find. Their values are also reported in Table X. Early extended-Huckel calculations predicted allowed porphyrin-to-metal charge-transfer excitations of the $a_{2u}(\pi) \rightarrow e_g(d_\pi)$ and $a_{2u}(\pi) \rightarrow a_{1g}(d_z2)$ as low as 1300 cm^{-1} above

Table X. Charge-Transfer Excitations of Fe(II)P with ^3E_g as the Reference (1000 cm^{-1})[a]

state	nature	configuration				energy		
		π	xy	z^2	x^2-y^2	INDO/CI	ab initio[b]	MSX-α[c]
				Fe(II)P				
^3E_g	ref	3	2	1	0	0.0	0.0	0.0
				$Fe(III)^+P^-$				
^5E_g	d_{xy}, $d_\pi \rightarrow e_g(\pi^*)$, $d_{x^2-y^2}$	2	1	1	1	24.8	9.4	
$^5B_{2g}$						27.4	19.0	
$^5A_{2g}$						27.6	19.0	
	$d_{x^2-y^2} \rightarrow e_g(\pi^*)$	3	1	1	0			
$^5A_{1g}$						28.1	19.0	
$^5B_{1g}$						28.3	19.0	
^5E_g	$d_\pi \rightarrow e_g(\pi^*)$	2	2	1	0		15.6	
^5E_g	d_{xy}, $d_\pi \rightarrow e_g(\pi^*)$, d_{z^2}	2	1	2	0		20.1	
^3E_g	$d_\pi \rightarrow e_g(\pi^*)$	2	2	1	0	27.6	18.6	12-16
^3E_g	d_{xy}, $d_\pi \rightarrow e_g(\pi^*)$, d_{z^2}	2	1	2	0			12-16
				$Fe(I)^-P^+$				
^3E_g	$e_g(\pi) \rightarrow d_{z^2}$	4	2	1	0	26.4		
$^3A_{1u}$	$a_{1u}(\pi) \rightarrow d_{z^2}$	4	2	1	0	34.8		
$^3A_{2u}$	$a_{2u}(\pi) \rightarrow d_{z^2}$	4	2	1	0	36.8		
^3E_u	$a_{2u}(\pi) \rightarrow d_\pi$	3	2	2	0			12-16

[a] Many of these configurations are mixed charge transfer and d → d. Only those that are identified as 50% or more charge transfer are given. [b] From Rawlings, Gouterman, Davidson, and Feller, ref 23. [c] From Sontum, Case, and Karplus, ref 24.

the $^3B_{2g}$ state.[41] Correcting this estimate by 0.63 ev from Table II suggests an excitation energy for $^3E_1$ ($a_{2u}(\pi) \rightarrow e_g(d_\pi)$) from the ^3E_g(A) state of about 18 000 cm^{-1}, not far from the estimate of Sontum et al. Although the present calculations show mixing of this charge-transfer state in the trip-triplets, it is only minor. We calculate the major components of these charge-transfer states to be above 35 00 cm^{-1}. In short the calculations do not agree with one another in the location of these charge-transfer bands. The prediction of such bands is particularly difficult as it requires not only an accurate description of the d orbitals, necessary for the d → d spectrum, and the ligand orbitals, necessary for an accurate representation of the $\pi \rightarrow \pi^*$ spectrum, but also the relative location of the d MOs and the ligand MOs. The relative ordering of these orbitals could be established by calculating the ionization spectrum, though we have not yet done this.

There are three possible explanations for the extra peaks observed at about 12 500 and 15 000 cm^{-1} in the spectrum of Fe(II)P. They are d → d excitations of the same spin multiplicity, or charge-transfer transitions, or spin-allowed components of the trip-triplets. All d → d excitations are g → g Laporte forbidden but might borrow intensity from near-lying ^3E_u bands (the Q band, for example) through vibronic interactions. Candidates from Table IV are the ^3E_g state calculated at 9300 cm^{-1} and the $^3A_{2u}$ calculated at 16 500 cm^{-1}. Charge-transfer excitations of the $^3A_{2u}$ or ^3E_g type are dipole allowed, but only $Fe(I)^-P^+$ states have low-energy states of this type, and we calculate those too high in energy. Low-lying states of the $Fe(III)^+P^-$ type are either spin and/or space forbidden. Our most likely candidates for the two observed features at 12 500 and 15 000 cm^{-1} are the trip-triplets of ^3E_u type. We note that the extended-Huckel calculations[41] and MSX-α calculations[24] favor allowed charge-transfer excitations at these energies.

5. Conclusions

We have considered the case of planar D_{4h} Fe(II) porphine, the simplest model compound for related systems or biological importance. Using the INDO method that we have found accurately reproduces the low-lying d → d transitions of atoms and ionic transition-metal complexes, we calculate the $^3A_{2g}$ (d^2_{xy}, d^2_π, $d^2_{z^2}$) lower in energy than the ^3E_g (d^2_{xy}, d^3_π, d_{z^2}) but by only 240 cm^{-1}. We have argued, however, on the basis of possible geometric considerations—each state having slightly different geometries—or on possible vibronic distortions of the ^3E_g state from D_{4h} symmetry—that states calculated so closely in energy could be reversed in actuality. We favor a lowest lying ^3E_g state as our calculated Mössbauer quadrupole splitting of +1.77 mm/s, for this state lies closest to the observed value of 1.5–1.6 mm/s and the experimental electron deformation maps on the analogous Fe(II) phthalocyanine is most readily comparable with this assignment.[37] In the calculation of the quadrupole coupling we note our success in achieving this value stems from a good deal of covalent mixing between the formally unoccupied $d_{x^2-y^2}$ orbital with the occupied ligand orbitals, considerably more than is found in the ab initio calculations that we review. Our calculated anisotropy in the population of the 4p orbitals is also greater than the ab initio calculations achieve and is similar to that obtained in MSX-α calculations; in our case this anisotropy has only a small effect on the calculated splitting. It has been suggested that the spin–orbital splitting of the lowest lying triplet state splits this state into a spin singlet ($S_x = 0$) at least 70 cm^{-1} below the spin doublet ($S_z = \pm 1$).[30,33] We would agree that this interaction is most likely through the X and Y components of the spin–orbit operator between the $^3A_{2g}$ and ^3E_g states (although the $^3B_{2g}$ state also lies close) but with the ^3E_g components lying lowest.

We have calculated the UV–visible excitations assuming quintet, triplet, and singlet ground states. The calculated spectra are discussed in detal in section 4, but we note that the calculations suggest that the spectra of the ^3E_g and $^3A_{2g}$ systems might be quite similar. The two extra features observed at about 12 500 and 15 000 cm^{-1} for these systems we associate with trip-triplets, porphyrin $\pi \rightarrow \pi^*$ triplets that have become spin allowed from the triplet ground state through spin coupling. The calculated positions of these bands are in better agreement with the reference ^3E_g calculation, although these bands are given considerably more oscillator strengths in the $^3A_{2g}$ calculation. Metal d → d transitions are also calculated in the visible, but they are all dipole forbidden, though they might vibrationally couple to the allowed transitions. Unlike earlier extended-Huckel calculations[41] we calculate no charge-transer excitations[24] in this region of the spectrum that are likely candidates.

Acknowledgment. We thank Dr. Marie-Madeleine Rohmer (University Louis Pasteur) and Dr. Ernest Davidson (Indiana University) for preprints of their papers (ref 25 and 23, respectively) before their publication.

This work was supported in part through research grants from the University of Florida, from the National Foundation of Cancer Research, and from a US Army Research Center Grant, No. DAAA15-85-C-0034.

M.C.Z. acknowledges with pleasure the hospitality of the Quantum Chemistry Group at the University of Uppsala, where some of this work was completed.

Registry No. Iron(II) porphine, 15213-42-0.

(41) Zerner, M. C.; Gouterman, M.; Kobayashi, H. *Theor. Chim. Acta* **1966**, *6*, 363. (1966).